

CLASSIFICATION CHANGED UNCLASSIFIED

naca Release form # 584
 authority of *H. L. Bryden* Date *June 27, 1951*
by HSR, 7-11-51

RESEARCH MEMORANDUM

A PRELIMINARY EXPERIMENTAL INVESTIGATION

OF A SUBMERGED CASCADE INLET

By R. Duane Christiani and Lauros M. Randall

Ames Aeronautical Laboratory
 Moffett Field, Calif.

CLASSIFICATION CANCELLED

Authority *J. W. Crawley* Date *12/14/53*
EO 10501

By *q# - 1-11-54* See *naca*
RF 1897

CLASSIFIED DOCUMENT

This document contains classified information affecting the National Defense of the United States within the meaning of the Espionage Act, USC 50-31 and 50-32. Its transmission or the revelation of its contents in any manner to an unauthorized person is prohibited by law. Information so classified may be imparted only to persons in the military and naval services of the United States, appropriate civilian officers and employees of the Federal Government who have a legitimate interest therein, and to United States citizens of known loyalty and discretion who of necessity must be informed thereof.

NATIONAL ADVISORY COMMITTEE
 FOR AERONAUTICS

WASHINGTON
 March 25, 1949

NACA RM No. A9A24

UNCLASSIFIED

RESTRICTED



UNCLASSIFIED

NATIONAL ADVISORY COMMITTEE FOR AERONAUTICS

RESEARCH MEMORANDUM

A PRELIMINARY EXPERIMENTAL INVESTIGATION

OF A SUBMERGED CASCADE INLET

By R. Duane Christiani and Lauros M. Randall

SUMMARY

An experimental investigation of a submerged air inlet incorporating a cascade of airfoils for turning and diffusing the entering air is described. The investigation was preliminary in nature and intended to be a guide for further research on this type inlet.

Variables associated with both NACA submerged air inlets and airfoil-cascade designs were considered. Modifications to the submerged inlet included changes to the ramp plan form and ramp angle. The cascade variables were: cascade-axis inclination, cascade-blade angle, solidity, and inclination of the center line of the duct aft of the cascade of airfoils.

For a cascade having a given number of blades and blade spacing, increasing the inclination of the cascade axis from 20° to 40° increased the maximum ram-pressure recovery for a given inclination of the duct center line and diffusion of the intake air. Increasing the solidity ratio of the cascade from 0 (no blades) to 2.00 (9 blades) increased the maximum ram-pressure recoveries obtained with large air deflections and reduced the maximum ram-pressure recoveries obtained with small air deflections.

The test results showed that for inlet-velocity ratios less than 1.0 an entrance ramp with curved diverging walls provided substantially higher ram-pressure recoveries than a ramp with parallel walls. The detrimental effect upon ram-pressure recovery of increasing ramp angle was found to be less for the submerged inlet with a cascade of airfoils than previous research had shown for the submerged inlet alone. Ramp angles between 8° and 10° appeared to be about optimum from considerations of ram-pressure recovery.

UNCLASSIFIED

INTRODUCTION

A cascade of airfoils may be employed to deflect an air stream with relatively small loss of available energy. With proper geometric arrangement, the deflection of the air stream is also accompanied by a considerable decrease in velocity.

As part of the program to study duct-inlet problems, an investigation was made to determine the feasibility of incorporating a cascade of airfoils as an integral part of a fully submerged intake. It was reasoned that, if an efficient cascade of airfoils were combined with an NACA submerged inlet (reference 1), the resultant air-induction system would diffuse and deflect the air in a minimum of space and still give a reasonable ram-pressure recovery.

The investigation discussed here was preliminary in nature and was meant to serve as a guide for future research. Only the more important variables of airfoil-cascade and submerged-inlet design were considered.

SYMBOLS

Symbols pertaining to the geometry of submerged cascade inlets are shown in figure 1. These symbols and others used in this report are defined as follows:

A_1	arbitrarily defined area of the inlet at station 1 ($A_1 = wl \sin \phi$), square feet
c	blade chord, feet
d	arbitrarily defined depth of the inlet at station 1 ($l \sin \phi$), feet
H	total pressure, pounds per square foot
ΔH	total-pressure loss, pounds per square foot
l	distance between the movable duct walls measured along the cascade axis, feet
p	static pressure, pounds per square foot
q	dynamic pressure, pounds per square foot

s	blade spacing measured parallel to cascade axis, feet
u	local air velocity in boundary layer, feet per second
U	local velocity outside boundary layer, feet per second
V	air velocity, feet per second
w	width of duct measured parallel to blade span, feet
α_0	cascade-blade angle (angle between the model center line and chord line of blades), degrees
β	ramp angle (acute angle between the model center line and the ramp center line), degrees
ϕ	cascade-axis angle (acute angle between the model center line and the cascade axis), degrees
γ	angle of the duct center line (acute angle between the duct center line and the center line of the model or fuselage), degrees
σ	solidity ratio of cascade of airfoils (c/s)
$\frac{H - P_0}{H_0 - P_0}$	ram-recovery ratio (ratio of free-stream ram pressure recovered to free-stream ram pressure)
V_1/V_0	inlet-velocity ratio

Subscripts

o	free stream
1	inlet station normal to model center line and passing through the intersection of the ramp and the contiguous duct wall (fig. 2)
2	duct station normal to duct walls and approximately 6 inches downstream of cascade axis (fig. 2)

MODEL AND APPARATUS

The submerged cascade inlet was installed on one side of a model

of a fuselage. No wing or tail surfaces were included on the model. Figure 3 shows the model mounted on two struts in one of the Ames 7- by 10-foot wind tunnels. The rear support strut served as part of the ducting system leading from the inlet to a variable-speed centrifugal blower outside the wind tunnel. The quantity of air drawn through the inlet was measured by an ASME standard orifice meter in the external ducting system. A schematic sketch of the fuselage, showing various model details and the path of the air drawn through the model, is presented in figure 2.

The width of the duct at and aft of the cascade was constant (6 in.) for all tests. Deflection of the cascade axis was obtained by rotation about a fixed point on the lip of the inlet. The distance between the movable duct walls measured along the cascade axis was held constant ($l = 8.34$ in.). The length of the ramp for the major portion of the investigation was 22.88 inches. Thus, for these conditions the ramp angle decreased with decreasing angle of the cascade axis. With the cascade-axis angle of 20° , the ramp angle was varied by decreasing the ramp length. The extent of the changes in ramp angle and width-to-depth ratio, for the cascade-axis angles tested, are given below:

Cascade-axis angle	Ramp angles	Width-to-depth ratio
20°	$7.9^\circ, 9.5^\circ$ $12^\circ, 15^\circ$	2.11
30°	10.6°	1.44
40°	13.7°	1.12

Ramps having both parallel and curved diverging walls were tested for several cascade arrangements. The coordinates for the curved diverging walls are given in figure 4.

The blades (airfoils) of the cascade had a chord of 1.50 inches and a span of 6 inches. The blade section, the RAF 27 superposed on a camber line consisting of a circular arc of 45.2° , was the same section as employed in the experiments reported by reference 2. The coordinates for this section are given in table I. The inlet design was such that the blade angle could be changed from 10° to 50° . The blades could be deflected about a point on the chord 37.5 percent from the leading edge. Solidity ratios of 0, 0.67,

1.00, and 2.00 could be obtained with 0, 3, 5, and 9 blades, respectively, evenly and symmetrically spaced along the cascade axis.

The walls of the duct aft of the cascade were parallel at all times. Two of these walls could be deflected through an angular range γ of from 15° to 70° with respect to the model center line. A pressure rake was approximately 6 inches behind the cascade, and the number of active tubes varied from 30 to 48 total-pressure tubes and from 3 to 5 static-pressure tubes, depending on the cascade-axis angle and the setting of the duct walls.

TESTS

Because the characteristics of a submerged cascade inlet are affected by both cascade and submerged-air-inlet design variables, the tests were logically divided into two parts. The cascade variables were investigated with a basic submerged air inlet having parallel ramp walls. These variables included cascade-axis angle ϕ , blade angle α_0 , solidity ratio σ , and angle of the duct center line γ . The variations of ramp angle and ramp plan form were tested for several cascade-blade angles with a representative cascade arrangement having a cascade-axis angle of 20° and a solidity ratio of 1.0. The extent of the investigation of the various parameters is given in table II.

Each modification was tested with several angles of the duct center line in order to bracket that for the maximum pressure recovery. The geometry of the model limited the minimum angle of the duct center line to 15° . With this limitation, it was not possible to obtain maximum pressure recovery for blade angles of 10° .

A range of inlet-velocity ratios from 0 to 1.4 was covered for all modifications tested. The fuselage remained at an angle of attack and an angle of sideslip of 0° . The tunnel airspeed was about 200 feet per second, which corresponds to a Reynolds number per foot of approximately 1,200,000.

The ram pressure recovered was measured aft of the cascade for the various angles of the duct center line and various diffusions provided by the aforementioned cascade and inlet variations. Ram-pressure recoveries were calculated from the average values of the duct total pressures as indicated by the rake.

A survey of the boundary layer over the fuselage at the

location of the duct entrance was made prior to the installation of the submerged cascade inlet. The boundary-layer profile is shown in figure 5.

No attempt was made to study or improve the flow at the junctions of the wall of the duct and the ramp and the wall of the duct and the lip. The inlet was designed so that alterations could be made quickly and the flow, no doubt, could be improved considerably for a fixed arrangement.

RESULTS AND DISCUSSION

General Considerations

Because of the number of variables in the geometry of air inlets, it is difficult to find a reference velocity ratio that is satisfactory for comparisons of all inlets and their modifications. An arbitrary velocity ratio V_1/V_0 has been chosen for the presentation of the results in this report because of its similarity to the inlet-velocity ratio normally used for presentation of results of submerged-inlet tests (reference 1). For a given inlet size and internal diffusion, therefore, the results presented herein can be compared to those of reference 1 at approximately the same inlet-velocity ratios V_1/V_0 . Since the distance between the movable duct walls for the submerged cascade inlet varied with the angles of the duct center line and the cascade axis, the diffusion or reduction of velocity of the entering air also varied with these angles for constant inlet-velocity ratios V_1/V_0 . For a given engine installation, therefore, a better evaluation of the effects of the parameters of the submerged cascade inlet may be obtained by comparison of the results for a given diffusion V_2/V_0 of the entering air.

The reduction of velocity of the air flowing through the duct was calculated in the following manner: For an incompressible fluid, the ratio of the velocity of the air behind the cascade of airfoils to the velocity of the same quantity of air passing through an area w_1 at station 1 is

$$\frac{V_2}{V_1} = \frac{\sin \phi}{\sin (\phi + \gamma)}$$

The ratio of the velocity of the air behind the cascade of airfoils to free-stream velocity is then

$$\frac{V_2}{V_0} = \frac{V_1}{V_0} \frac{V_2}{V_1} = \frac{V_1}{V_0} \frac{\sin \phi}{\sin (\phi + \gamma)}$$

The relation between these variables is shown in figure 6 for several inclinations of the cascade axis.

The test results were obtained by measuring the ram-pressure recovery for various angles of the center line of the duct and for various constant inlet-velocity ratios. Typical examples of these data are shown in figure 7 for the inlet having a ramp with parallel walls, a ramp angle of 7.9° , a cascade-axis angle of 20° , a solidity ratio of 1.0, and cascade-blade angles of 10° , 20° , 30° , and 40° . The maximum ram-pressure recoveries for a given inlet-velocity ratio are well defined for most blade angles, with a considerable reduction of ram-recovery ratio for angles of the duct center line on either side of the optimum.

The values of the maximum ram-recovery ratios obtained with each blade angle for all modifications tested are presented in table III, together with the angles of the duct center line for which these maximum ram-recovery ratios were obtained. It is believed that the maximum pressure recoveries for a given blade angle resulted when the walls of the duct were parallel to the mean direction of air flow leaving the blades. A few directional-pitot surveys made behind the blades indicated this to be generally true. With the angle of the duct center line greater or less than the optimum for a given blade angle, the pressure losses were greater, probably because the air leaving the cascade of airfoils was directed toward one wall of the duct and away from the other. Reference 3 indicates that "secondary flow" occurs with a cascade of airfoils because of the boundary layer on the walls of the duct at the ends of the blades and the pressure difference between the upper and lower surface of adjacent blades. Aside from the losses that would normally be encountered at the entrance to a submerged inlet (reference 1), this secondary flow would also affect the pressure recovery. However, the origin of the losses obtained with the modifications tested has not been completely established.

As indicated by figure 7, the ram-recovery ratios of table III were not necessarily the maximum ram-recovery ratios for the given angles of the duct center line. It is evident that for a given inlet-velocity ratio an envelope of the curves for various blade angles represents the maximum value of ram-recovery ratio attainable with the type of inlet used for a given angle of the duct center line.

To summarize the results of the tests with various modifications of the inlet, the envelopes of the curves of maximum ram-recovery ratio obtained for the range of angles of the duct center line investigated were determined for various inlet-velocity ratios. These results are presented in figures 8 to 10. The points of tangency of the envelope curves with the curves representing the variation of ram-recovery ratio with angle of the duct center line for constant blade angles are indicated by the intersections of the dashed lines with the envelope curves. For a given angle of the duct center line, as would be the case for a normal installation, it is evident that the optimum blade angle varied somewhat with inlet-velocity ratio.

The inlet-velocity ratio for maximum ram-recovery ratio was not established for all modifications of the inlet tested. The range of inlet-velocity ratios investigated was considered adequate for this preliminary investigation; it was limited by the size of model, the capacity of the compressor supplying the auxiliary air, and the required accuracy of the data.

Cascade Modifications

Solidity ratio.— The envelope curves giving the variation of maximum ram-recovery ratio with angle of the duct center line for solidity ratios of 0, 0.67, 1.00, and 2.00 are shown in figure 8. These data were obtained with the ramp having parallel walls, a ramp angle of 7.9° , and a cascade-axis angle of 20° .

As shown by the data of figure 8, increasing the solidity ratio from 0 to 0.67 gave higher ram-recovery ratios for all angles of the duct center line tested, particularly for those angles greater than 30° . Increasing the solidity ratio from 0.67 to 1.00 generally provided a slight increase of ram-recovery ratio for duct center-line angles greater than 40° . Further increase of solidity ratio from 1.00 to 2.00 gave detrimental effects for small angles of the duct center line and large inlet-velocity ratios but increased the ram-recovery ratios for the largest angles of the duct center line investigated.

It is apparent from these data that the solidity ratio for maximum ram-pressure recovery increased with increasing angle of the duct center line. For a fixed blade chord, the optimum solidity ratio should increase with air deflection up to the point where the pressure losses provided by the increasing number of blades offset the increased turning efficiency. The optimum solidity ratio was

not established for the larger air deflections by the conditions tested.

Cascade-axis angles.— The envelope curves of the maximum ram-recovery ratios obtained with cascade-axis angles of 20° , 30° , and 40° are shown in figure 9. The data were obtained with the ramp having parallel walls and a cascade solidity ratio of 1.0. As the angle of the cascade axis increased from 20° to 40° , the entrance width-to-depth ratio decreased from 2.05 to 1.09 and the ramp angle increased from 7.9° to 13.7° because of the mechanics of the model. It was found in reference 1 that variations of entrance width-to-depth ratio within this range had only a small effect on ram-recovery ratio for a submerged inlet with parallel ramp walls. As will be shown later, variation of ramp angle within the range encountered had only a small effect.

The results presented in figure 9 indicate that for a given angle of the duct center line the maximum ram-pressure recoveries increased with increasing angle of the cascade axis. For an angle of the duct center line of 40° and an inlet-velocity ratio of 0.6, increasing the angle of the cascade axis from 20° to 40° increased the maximum ram-recovery ratio from 0.50 to 0.65. The ratios of the velocity of the air aft of the cascade to that of the free-stream air for these two conditions were 0.24 and 0.39, respectively. For constant values of inlet-velocity ratio and angle of the duct center line the amount that the air was diffused in passing through the cascade decreased as the cascade-axis angle increased. This reduction of diffusion at the higher cascade-axis angles would provide a smaller pressure rise across the cascade and should reduce the pressure losses.

To provide a more equitable comparison for a given engine installation, results which illustrate the effect of cascade-axis angle on the maximum ram-pressure recoveries obtained for a given diffusion have been tabulated. For a ratio of the velocity aft of the cascade to free-stream velocity V_2/V_0 of 0.3 and an angle of the duct center line of 40° , the following results were obtained:

ϕ	V_1/V_0	Maximum ram-recovery ratio
20°	0.76	0.52
30°	.56	.58
40°	.46	.60

Similar results were obtained for other diffusions and angles of the duct center line. It is noted that the largest angles of the cascade axis tested provided the highest ram-recovery ratios.

Submerged-Entrance Modifications

Two important design parameters which affect the aerodynamic characteristics of submerged-type air inlets are ramp plan form and ramp angle, as has been indicated in reference 1. The effects of these two geometrical changes on the characteristics of a submerged inlet utilizing a cascade of airfoils were investigated. A solidity ratio of 1.0 and a cascade-axis angle of 20° were chosen for the investigation.

Ramp plan form.— Previous research on submerged inlets has shown that at the lower inlet-velocity ratios curved divergent ramp walls effected substantial gains in ram-pressure recovery over that attainable with parallel ramp walls. Figure 10 shows this characteristic to be true also for a cascade inlet. For an angle of the duct center line of 40° and an inlet-velocity ratio of 0.6, the inlet with parallel ramp walls provided a ram-recovery ratio of 0.50, while the inlet with curved divergent ramp walls provided a ram-recovery ratio of 0.69.

Ramp angle.— The ramp angle of the submerged cascade inlet was varied for ramps having both parallel and curved divergent walls. The angles of the duct center line tested, however, did not cover a sufficient range to establish the maximum ram pressures available for all cascade blade angles and ramp angles. The maximum ram-pressure recoveries attainable for any angle of the duct center line, therefore, were not ascertained. Test results are presented in figures 11 and 12, however, for three blade angles and the test angles of the duct center line that most nearly represented those for maximum ram-pressure recovery. The results are given as the variation of ram-recovery ratio with inlet-velocity ratio for ramp angles of 7.9° , 9.5° , 12.0° , and 15.0° for the inlet with parallel ramp walls (fig. 11) and the inlet with curved divergent ramp walls (fig. 12).

From consideration of ram-pressure recovery, an entrance ramp angle between 8° and 10° appeared to be about optimum for the submerged cascade inlet. The highest ram-recovery ratio measured for an angle of the duct center line of 40° and an inlet-velocity ratio of 0.6 was 0.73. This value was obtained with a ramp angle of 9.5° , a blade angle of 30° , and a ramp having curved diverging walls (fig. 12). The results previously discussed have indicated, however,

that the cascade arrangement used in the study of the effects of ramp angle was not necessarily optimum.

It is noted that changing ramp angle had a greater effect on the ram-pressure recoveries for the inlet with divergent ramp walls, this result being similar to that observed in reference 1. However, the decrease in ram-pressure recovery at the higher ramp angles was considerably less for the submerged cascade inlet than for the submerged inlet without the cascade. It is possible that the cascade had an effect similar to a screen in a divergent duct (reference 4) and reduced the tendency toward flow separation on the ramp. Further, increasing the ramp angle should tend to decrease the angle of attack of the blades. This could have resulted in more efficient turning of the air by the blades and partially offset the detrimental effect of increasing ramp angle found for a submerged inlet without the cascade of airfoils.

CONCLUDING REMARKS

The results of this preliminary investigation of submerged cascade inlets indicate sufficient promise to warrant more extensive research. From considerations of ram-pressure recovery it was found that the airfoil cascade was especially promising for large amounts of turning and diffusion of the entering air. However, the ram-recovery ratios for these conditions were not as high as desirable. With further development of this type of inlet and a study of the origin of the pressure losses it should be possible to increase the ram-pressure recovery. The submerged inlet utilizing a cascade of airfoils should then be satisfactory for certain air-induction installations where space is at a premium and short internal ducting is desirable.

Analysis of the results indicates the important ranges of the variables investigated. In general, it was found that the solidity ratio for maximum ram-pressure recovery increased with increasing angle of the duct center line. Increasing the angle of the cascade axis from 20° to 40° increased the maximum ram-pressure recoveries obtained for a given angle of the duct center line and diffusion. An entrance ramp having curved divergent walls provided higher ram-pressure recoveries throughout the important range of inlet-velocity ratios than one with parallel walls. Ramp angle had a smaller effect on the ram-pressure recoveries for the submerged cascade inlet than it did for a submerged inlet without the cascade. An entrance ramp angle between 8° and 10° appeared to be about optimum for the submerged cascade inlet from ram-pressure-recovery considerations.

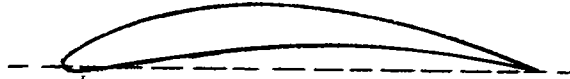
A ram-recovery ratio of 0.73 was obtained for an angle of the duct center line of 40° and diffusion of 4.23 to 1.00 with an inlet-velocity ratio of 0.6. The inlet arrangement for this condition had a cascade-axis angle of 20° , a solidity ratio of 1.0, a blade angle of 30° , an entrance ramp with curved divergent walls, and a ramp angle of 9.5° . The test results indicated, however, that these conditions were not necessarily optimum.

Ames Aeronautical Laboratory
National Advisory Committee for Aeronautics
Moffett Field, Calif.

REFERENCES

1. Mossman, Emmet A., and Randall, Lauros M.: An Experimental Investigation of the Design Variables for NACA Submerged Duct Entrances. NACA RM No. A7I30, 1948.
2. Harris, R. G., and Fairthorne, R. A.: Wind-Tunnel Experiments with Infinite Cascades of Aerofoils. R.&M. 1206, British A. R. C. (1928)
3. Carter, A. D. S., and Cohen, Elizabeth M.: Preliminary Investigation into the Three Dimensional Flow through a Cascade of Aerofoils. Power Jets, Ltd., Rep. No. R-1180. (1946)
4. McLellan, C. H., and Nichols, R. M.: An Investigation of Diffuser-Resistance Combinations in Duct Systems. NACA ARR, Feb. 1942.

TABLE I.- CASCADE-BLADE COORDINATES



R.A.F. 27 PROFILE SUPERPOSED ON A
45.2° CIRCULAR - ARC CAMBER LINE.

UPPER SURFACE		LOWER SURFACE	
STATION % CHORD	ORDINATE % CHORD	STATION % CHORD	ORDINATE % CHORD
0	0	0	0
.7	1.76	.7	-.56
2.9	3.67	2.9	-.80
6.4	5.85	6.4	-.51
11.3	8.21	11.3	.30
17.2	10.42	17.2	1.33
24.1	12.27	24.1	2.56
31.8	13.68	31.8	3.78
40.2	14.41	40.2	4.83
49.1	14.44	49.1	5.56
57.7	13.67	57.7	5.85
66.6	12.23	66.6	5.71
74.9	10.21	74.9	5.06
82.8	7.70	82.8	3.98
89.6	5.07	89.6	2.64
95.4	2.51	95.4	1.17
100.0	0	100.0	0
L.E. RADIUS 0.75% CHORD			



TABLE II.— SUMMARY CHART OF ALL VARIABLE INVESTIGATED

	σ	ϕ	β	α_0	γ
Solidity ratio (σ)	2.0	20°	7.9°	10° to 40°	20° to 55°
	1.0	20° to 40°	7.9° to 15°	10° to 50°	15° to 55°
	0.66	20°	7.9°	10° to 40°	20° to 50°
Cascade — axis angle (ϕ)	0.66 to 2.0	20°	7.9° to 15°	10° to 50°	20° to 55°
	1.0	30°	10.6°	20° to 40°	20° to 50°
	1.0	40°	13.7°	10° to 30°	15° to 40°
Ramp angle (β)	0.66 to 2.0	20° to 40°	7.9°	10° to 50°	15° to 55°
	1.0	20°	9.5°	20° to 40°	20° to 50°
	1.0	20°	12.0°	20° to 40°	20° to 50°
	1.0	20°	15.0°	20° to 40°	20° to 50°
Parallel ramp walls	0.66 to 2.0	20° to 40°	7.9° to 15°	10° to 50°	15° to 55°
Divergent ramp walls	1.0	20°	7.9° to 15°	20° to 40°	20° to 55°



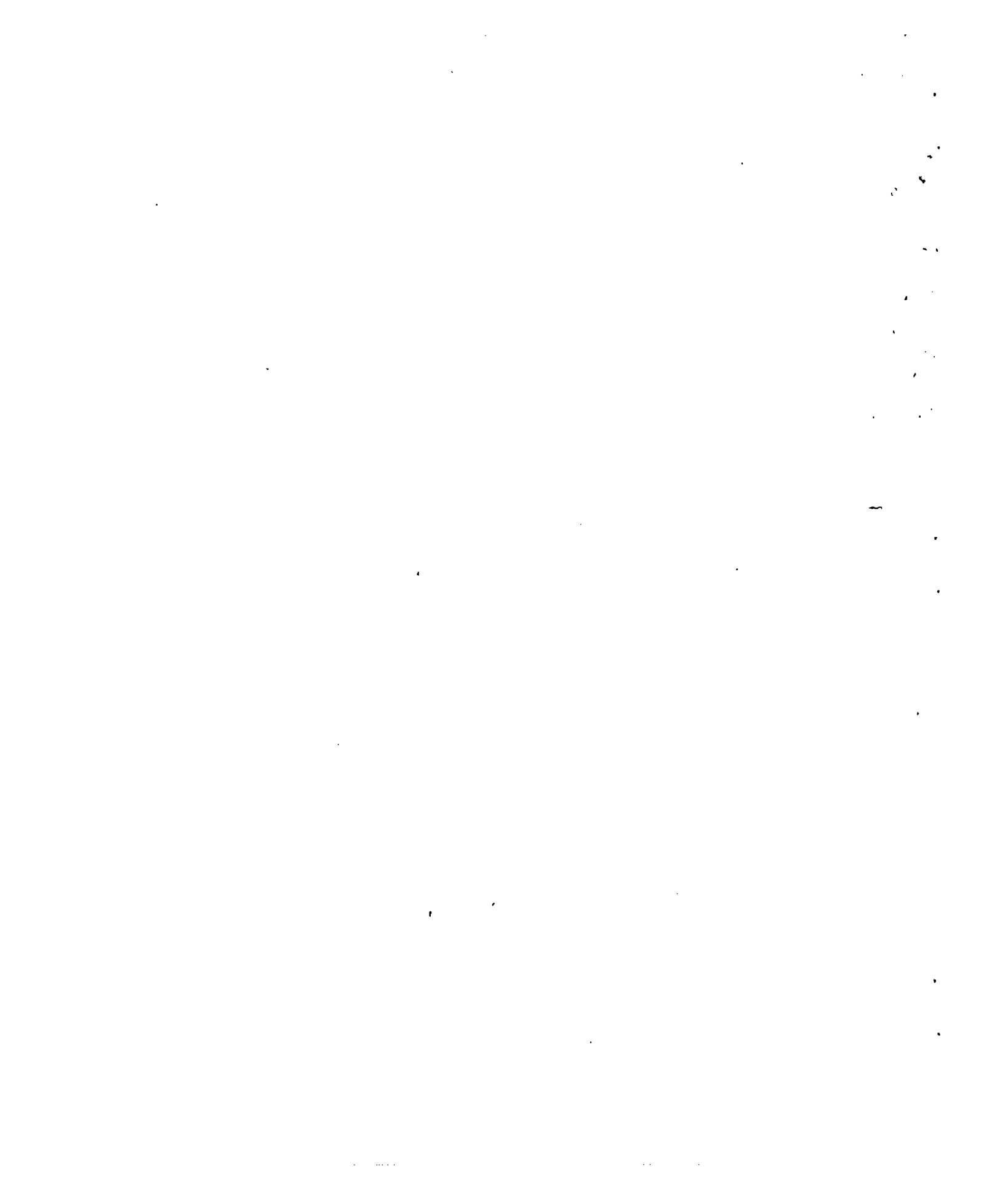
TABLE III.— MAXIMUM RAM-RECOVERY RATIOS OBTAINED WITH GIVEN
BLADE ANGLES FOR VARIOUS INLET ARRANGEMENTS

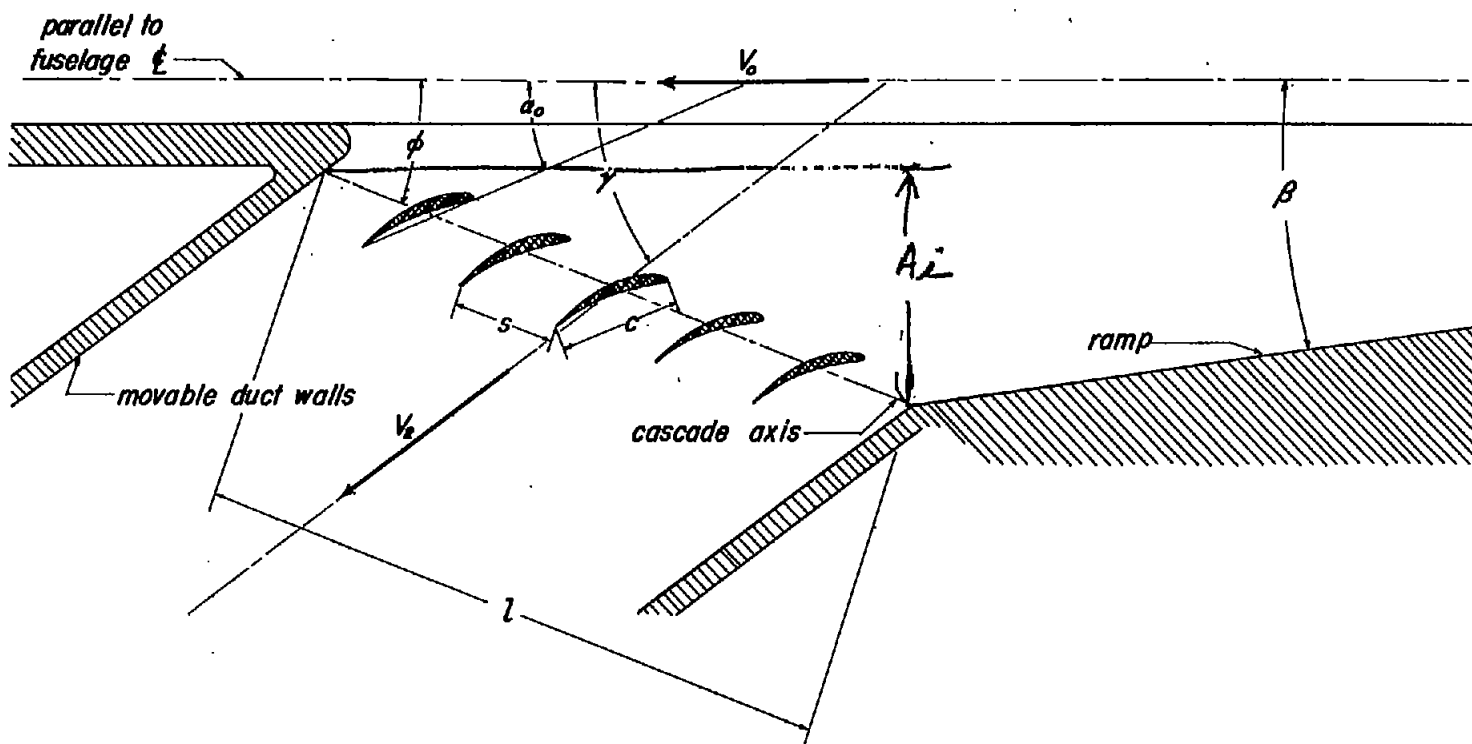
Configuration	V_1/V_0	$\alpha_0, 10^\circ$		$\alpha_0, 20^\circ$		$\alpha_0, 30^\circ$		$\alpha_0, 40^\circ$	
		γ^a (deg)	$\frac{H_2 - P_0}{H_0 - P_0}$	γ^a (deg)	$\frac{H_2 - P_0}{H_0 - P_0}$	γ^a (deg)	$\frac{H_2 - P_0}{H_0 - P_0}$	γ^a (deg)	$\frac{H_2 - P_0}{H_0 - P_0}$
$\phi, 20^\circ; \sigma, 0.67;$ parallel ramp walls	0.2	10	.59 ^b	21	.52	26	.49	37	.46
	.6	13	.69 ^b	23	.59	29	.55	40	.49
	1.0	15	.79 ^b	25	.71	31	.64	41	.57
	1.4	15	.84 ^b	25	.80	32	.73	41	.64
$\phi, 20^\circ; \sigma, 1.0;$ parallel ramp walls	.2	7	.62 ^b	17	.55	25	.51	40	.45
	.6	11	.70 ^b	22	.59	28	.55	42	.47
	1.0	14	.78 ^b	25	.69	31	.62	45	.52
	1.4	15	.76	25	.78	32	.70	45	.59
$\phi, 20^\circ; \sigma, 2.0;$ parallel ramp walls	.2	7	.60 ^b	20	.55	27	.51	42	.44
	.6	11	.66 ^b	24	.62	31	.55	45	.45
	1.0	12	.60 ^b	25	.66	33	.62	47	.48
	1.4	13	.45 ^b	27	.71	35	.67	50	.54
$\phi, 30^\circ; \sigma, 1.0;$ parallel ramp walls	.2	--	--	15	.56	25	.53	35	.49
	.6	--	--	19	.67	29	.63	40	.53
	1.0	--	--	22	.79	31	.75	43	.59
	1.4	--	--	23	.84	32	.80	45	.64
$\phi, 40^\circ; \sigma, 1.0;$ parallel ramp walls	.2	10	.54 ^b	18	.53	25	.52	--	--
	.6	15	.77	21	.71	29	.67	--	--
	1.0	17	.87	23	.84	31	.80	--	--
$\phi, 20^\circ; \sigma, 1.0;$ curved divergent ramp wall	.2	--	--	26	.68	35	.68	47	.62
	.6	--	--	29	.74	37	.70	50	.58
	1.0	--	--	31	.73	40	.71	51	.58
	1.4	--	--	31	.70	41	.70	52	.58

^aAngle of the duct center line for maximum ram-recovery ratio.

^bThe maximum ram-recovery ratios were obtained by extrapolation of test results.







α_0 — Blade angle

β — Ramp angle

γ — Angle of duct center line

ϕ — Cascade-axis angle

c — Cascade-blade chord

l — Length along cascade axis

s — Cascade-blade spacing

V_0 — Free-stream air velocity

V_2 — Duct air velocity



Figure 1.— Symbols for submerged cascade inlets.

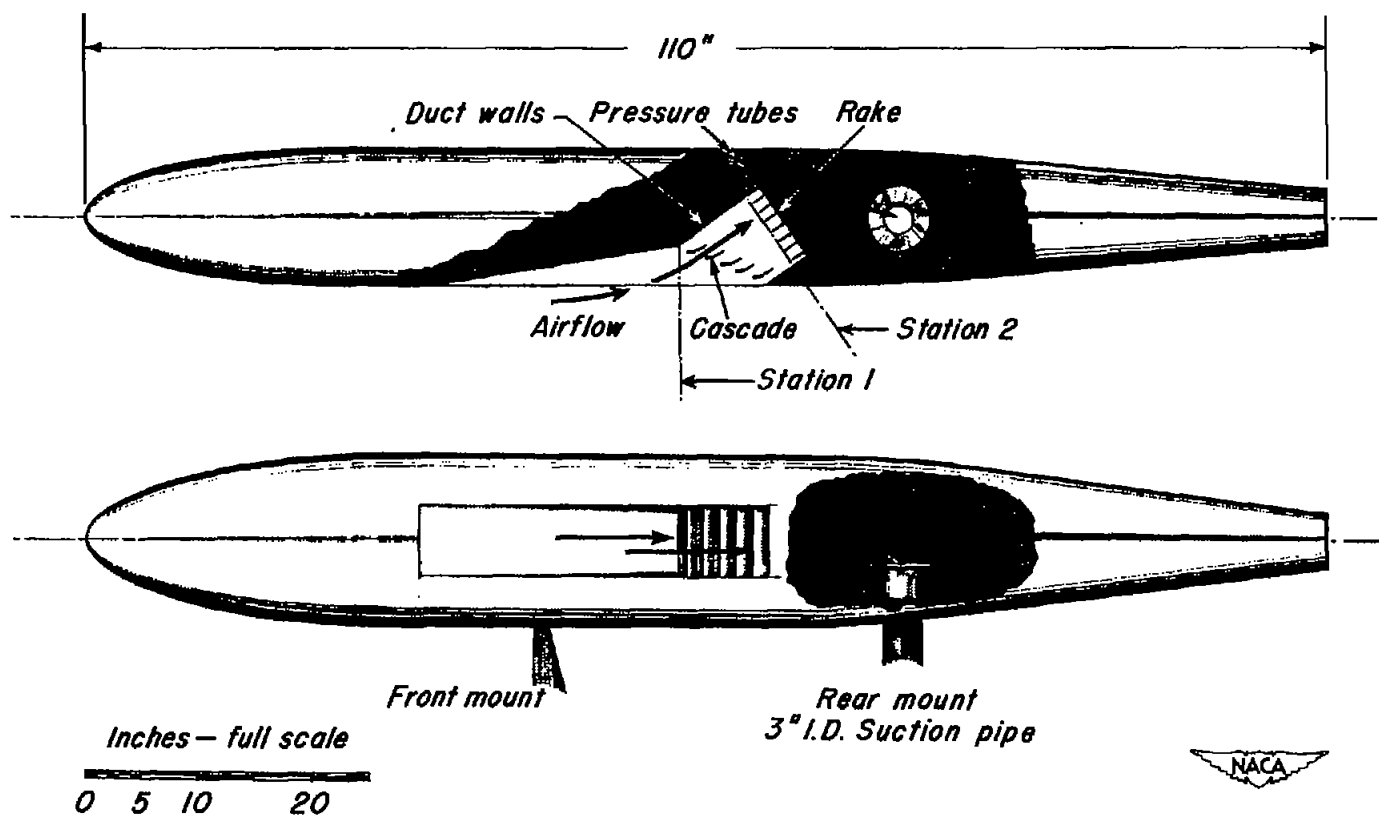


Figure 2.- Model installation and air-flow diagram for the submerged cascade inlet.

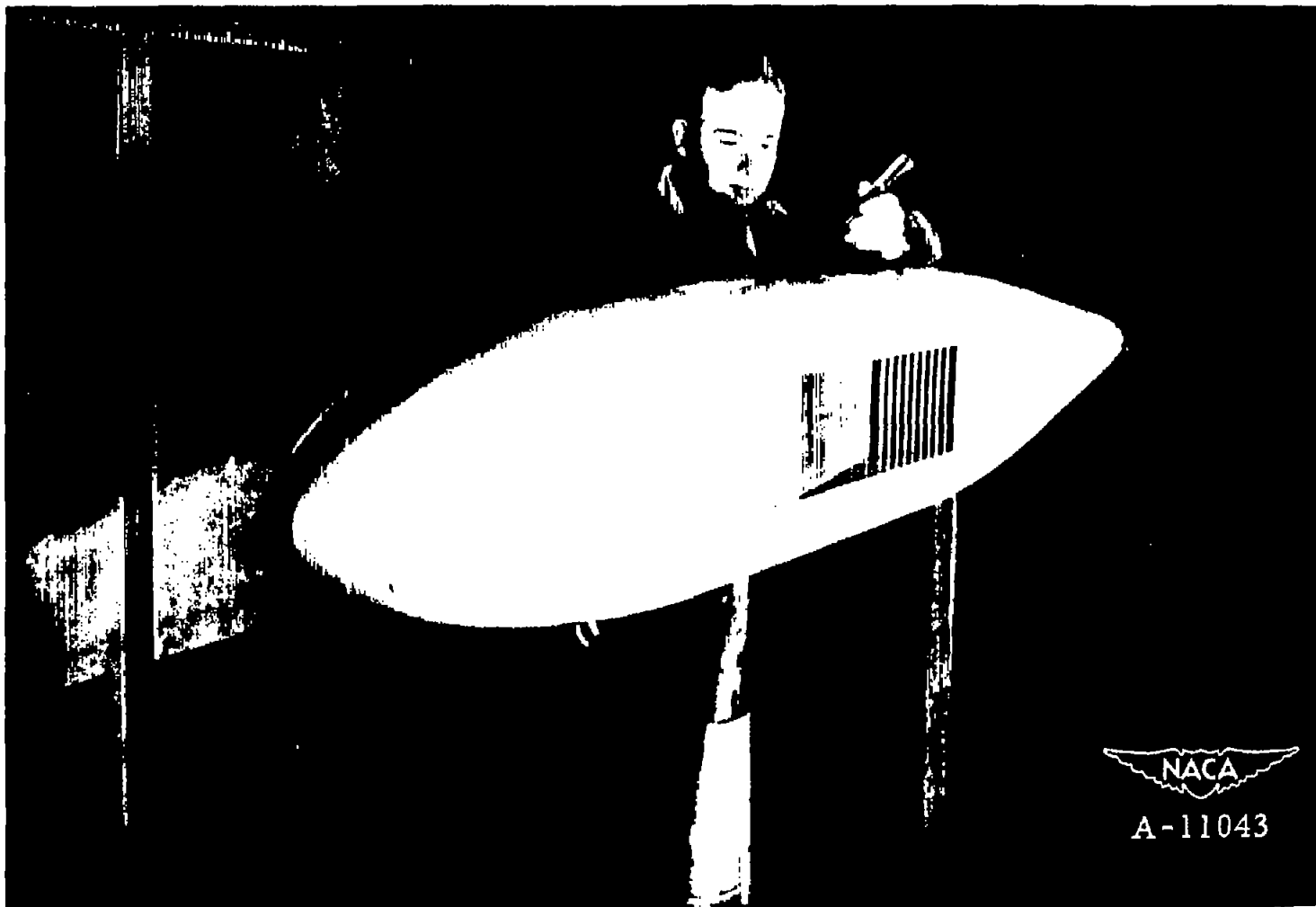
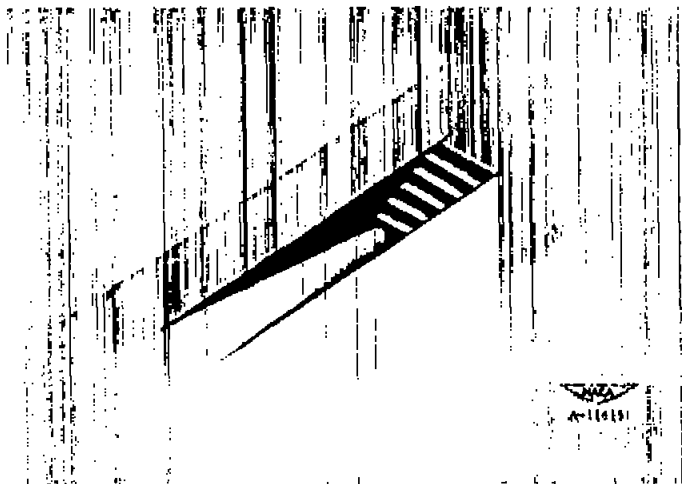
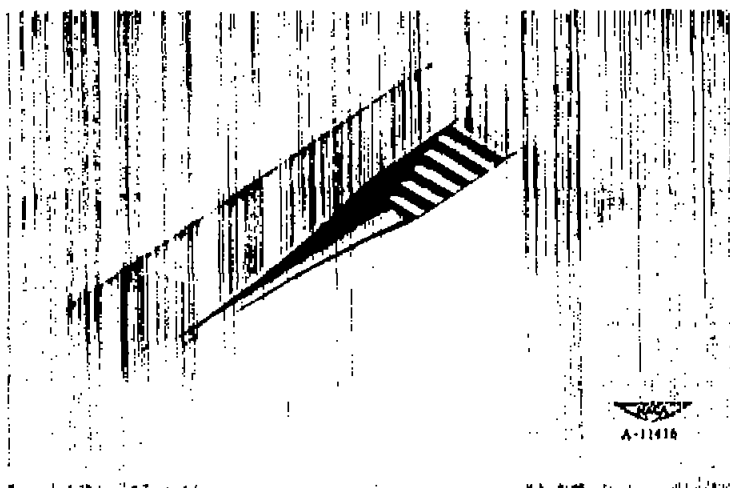
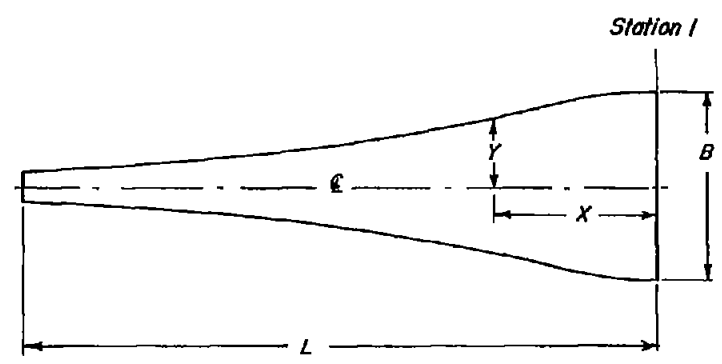


Figure 3.-- The model mounted in one of the Ames 7- by 10-foot wind tunnels.





(a) Parallel ramp walls.



(b) Curved divergent ramp walls.

x/L	y/B	x/L	y/B
0	0.500	0.50	0.196
0.05	.493	.60	.152
.10	.467	.70	.114
.20	.387	.80	.081
.30	.309	.90	.058
.40	.245	1.00	.044

(c) Curved divergent ramp-wall coordinates.

Figure 4.— Ramp plan forms tested.



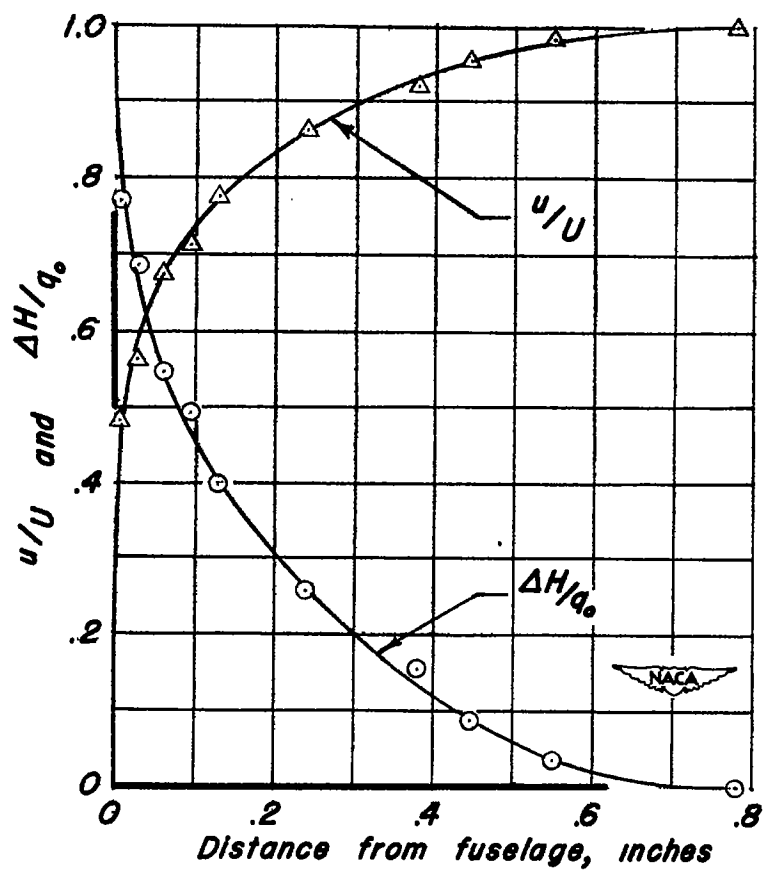


Figure 5.— Characteristics of the fuselage boundary layer at the lip station with the inlet removed.

$$\frac{V_e}{V_0} = \frac{V_i \left[\frac{\sin \phi}{\sin(\phi + \gamma)} \right]}$$

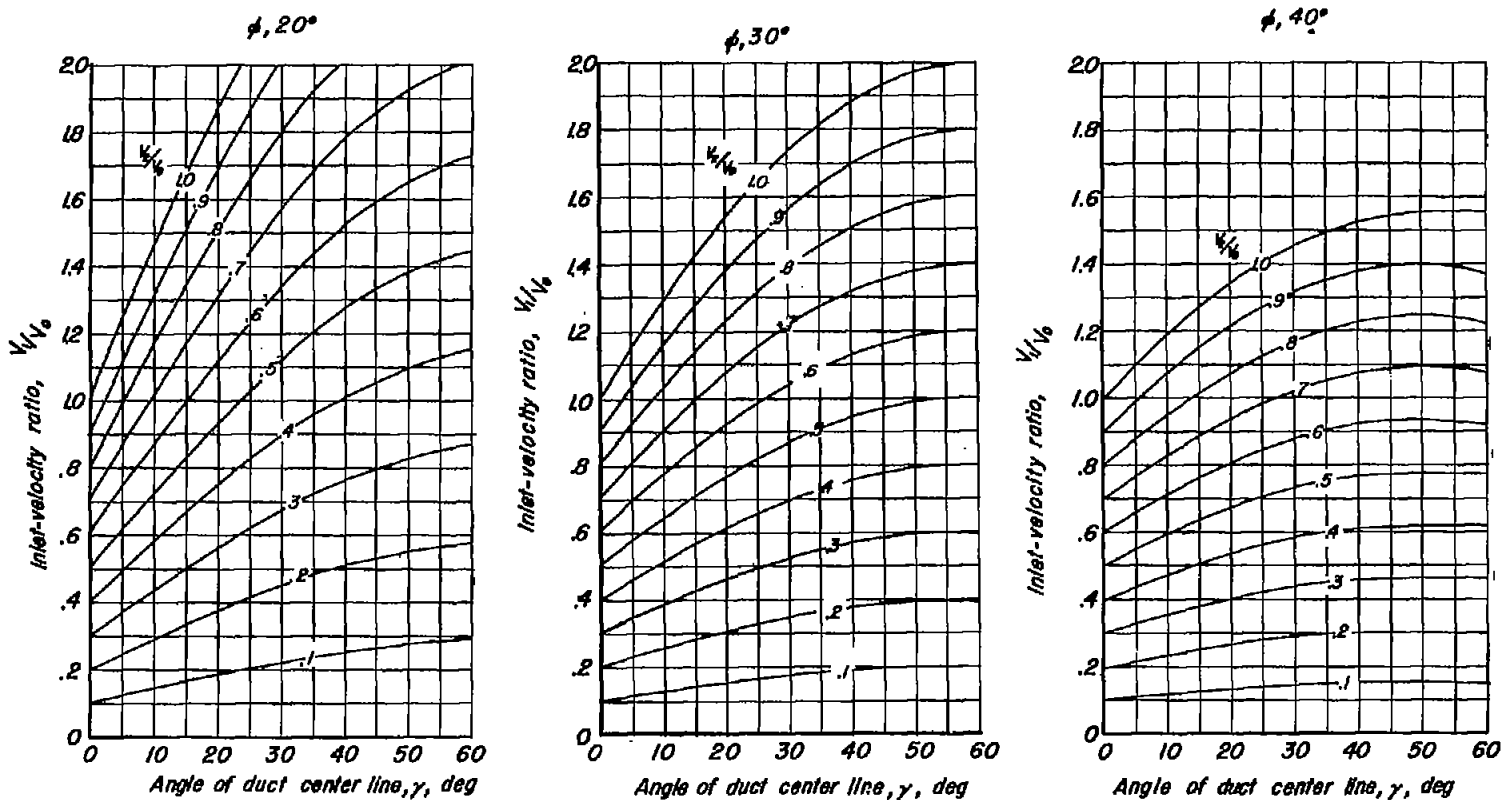
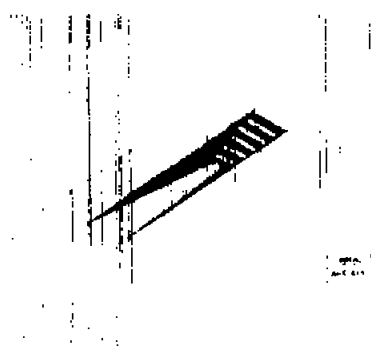
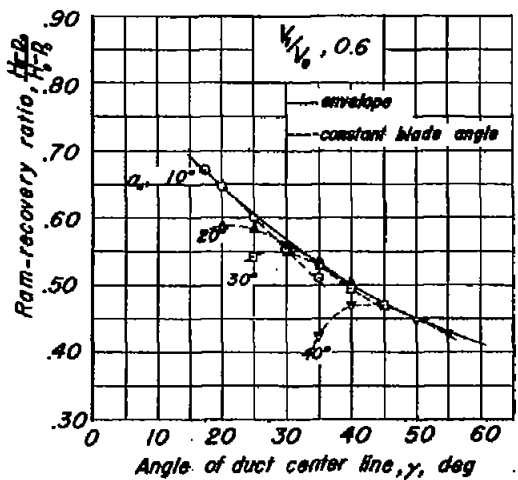


Figure 6.— Computed variation of inlet-velocity ratio with angle of duct center line for constant diffusion.



Parallel ramp walls

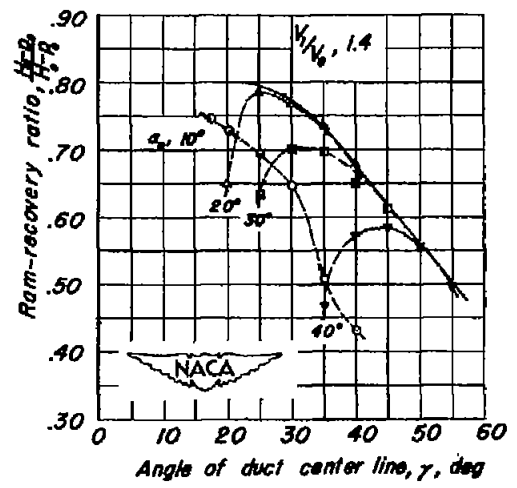
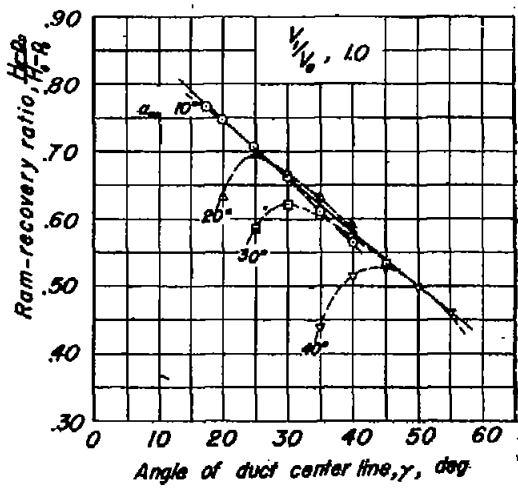


Figure 7.— Variation of ram-recovery with angle of duct center line for several cascade-blade angles and inlet-velocity ratios; $\phi, 20^\circ$; $\sigma, 1.0$; $\beta, 7.9^\circ$

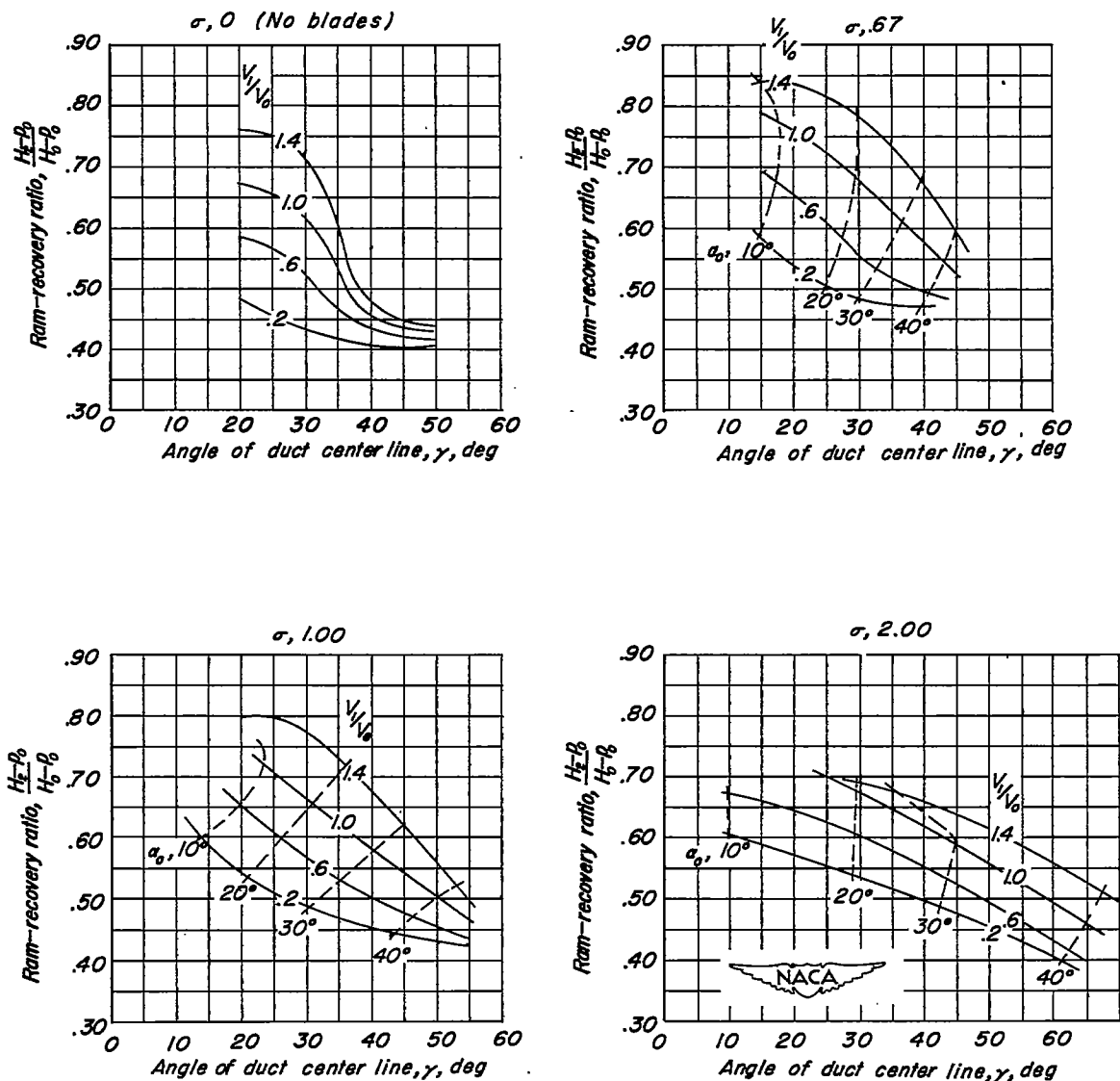


Figure 8.— Variation of maximum ram-recovery ratio with angle of duct center line for four solidity ratios with parallel ramp walls. $\phi, 20^\circ$; $\beta, 7.9^\circ$

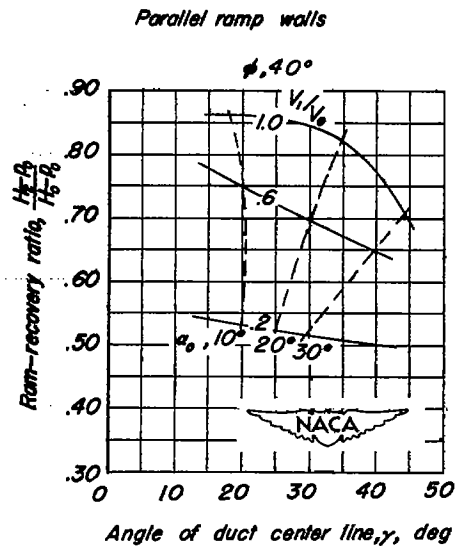
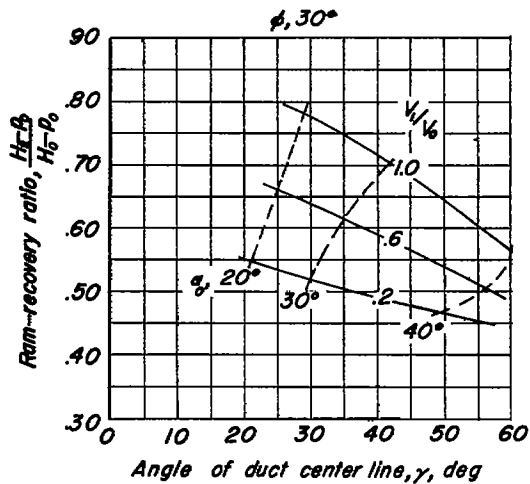
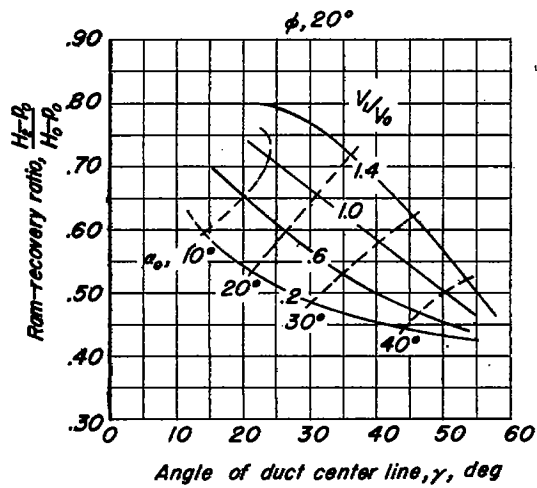
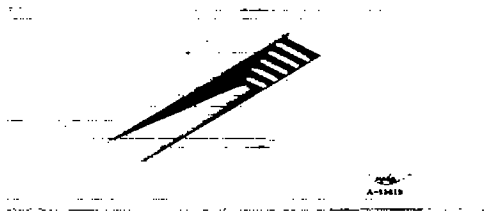
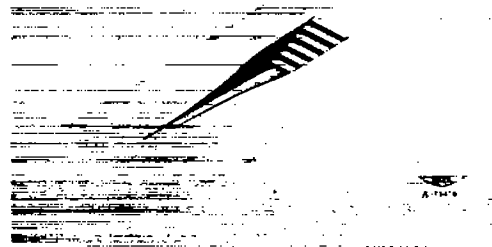


Figure 9.— Variation of maximum ram-recovery ratio with angle of duct center line for three angles of the cascade axis, $\sigma, 1.0$.



Parallel ramp walls



Curved divergent ramp walls

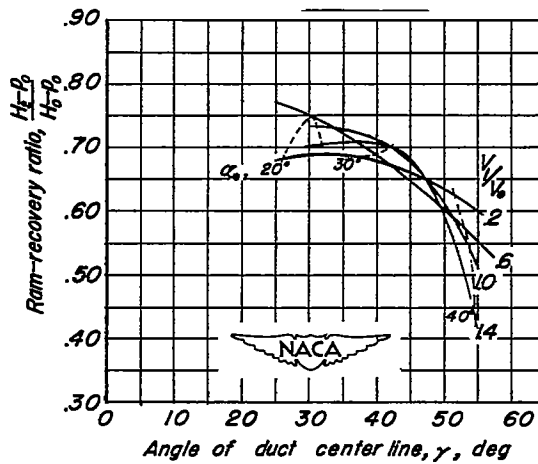
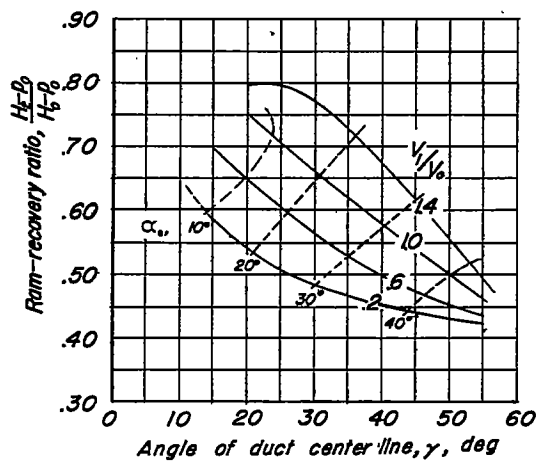
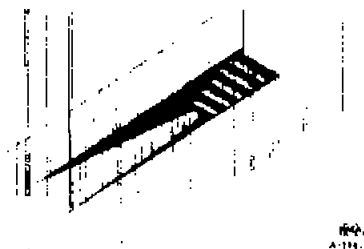
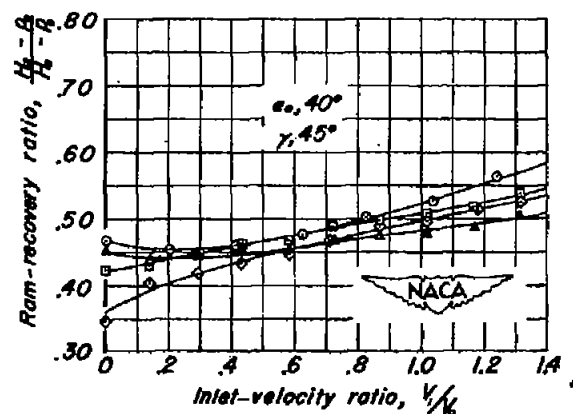
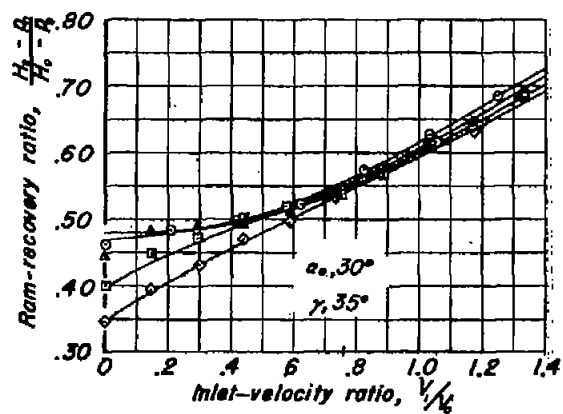
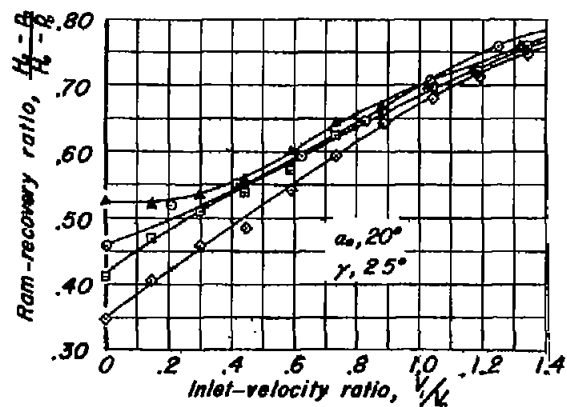
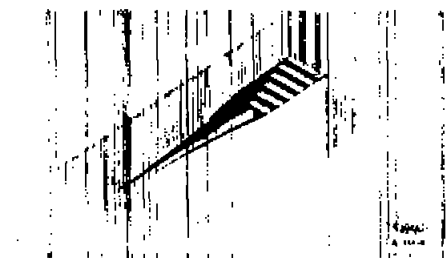
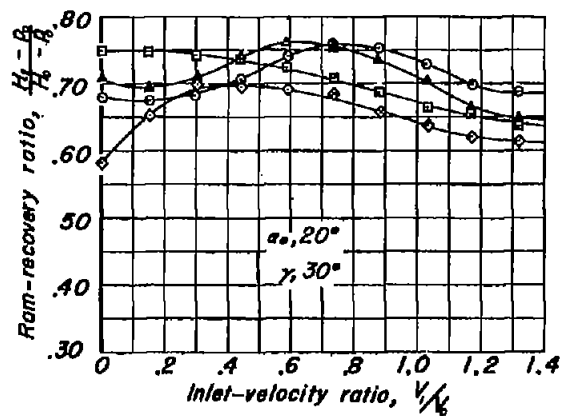


Figure 10.— Variation of maximum ram-recovery ratio with angle of duct center line for parallel and curved divergent ramp walls. $\phi, 20^\circ$; $\sigma, 1.0$; $\beta, 7.9^\circ$.



Symbols	Ramp angle, β
○	7.5°
△	9.5°
□	12.0°
◇	15.0°

Figure 11.— The effect of ramp angle on the variation of ram-recovery ratio with inlet-velocity ratio for the ramp with parallel walls. $\phi, 20^\circ$; $\sigma, 1.0$.



Symbols	Ramp angle, β
○	7.9°
△	9.5°
□	12.0°
◇	15.0°

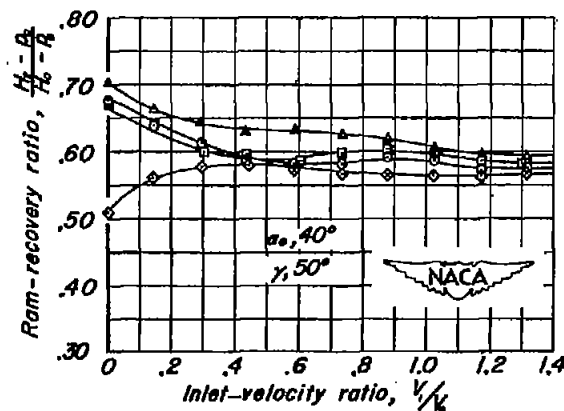
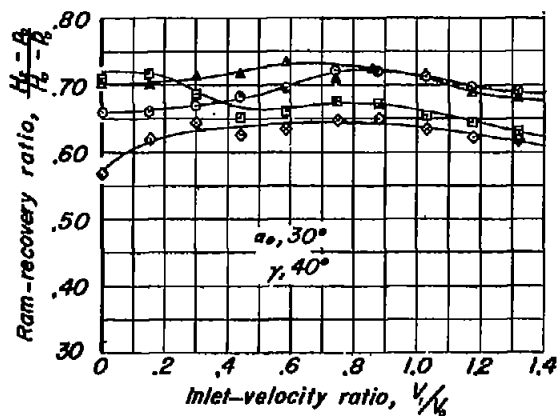


Figure 12.— The effect of ramp angle on the variation of ram-recovery ratio with inlet-velocity ratio for the ramp with curved divergent walls. $\phi, 20^\circ$; $\sigma, 1.0$.

NASA Technical Library



3 1176 01434 4718

DF
J-26-49